Radiology

Focused Ultrasound Hyperthermia for Targeted Drug Release from Thermosensitive Liposomes: Results from a Phase I Trial

Michael D. Gray, PhD • Paul C. Lyon, DPhil • Christophoros Mannaris, PhD • Lisa K. Folkes, DPhil • Michael Stratford, PhD • Leticia Campo, Dip • Daniel Y. F. Chung, FRCR • Shaun Scott, FRCA • Mark Anderson, FRCR • Robert Goldin, FRCPath • Robert Carlisle, PhD • Feng Wu, PhD • Mark R. Middleton, FRCP • Fergus V. Gleeson, FRCR • Constantin C. Coussios, PhD

From the Institute of Biomedical Engineering, University of Oxford, Old Road Campus Research Building, Oxford OX3 7DQ, England (M.D.G., P.C.L., C.M., R.C., C.C.C.); Nuffield Department of Surgical Sciences, John Radcliffe Hospital, Oxford University Hospitals NHS Foundation Trust, Oxford, England (P.C.L., F.W.); Departments of Radiology (P.C.L., D.Y.F.C., M.A., F.V.G.) and Oncology (M.R.M.), Churchill Hospital, Oxford University Hospitals NHS Foundation Trust, Oxford, England; Department of Oncology, CRUK/MRC Oxford Institute for Radiation Oncology, University of Oxford, Oxford, England (L.K.F., M.S., L.C.); Nuffield Department of Anaesthetics, Oxford University Hospitals Foundation NHS Trust, Oxford, England (S.S.); and Centre for Pathology, Faculty of Medicine, Imperial College London, London, England (R.G.). Received June 19, 2018; revision requested August 23; final revision received October 27; accepted November 20. **Address correspondence to** C.C.C. (e-mail: *constantin.coussios@eng.ox.ac.uk*).

Supported by the Oxford Biomedical Research Centre, National Institute for Health Research, the Oxford Centre for Drug Delivery Devices (programme grant EP/L024012/1), and the Engineering and Physical Sciences Research Council.

Conflicts of interest are listed at the end of this article.

See also the editorial by Dickey and Levi-Polyachenko in this issue.

Radiology 2019; 291:232–238 • https://doi.org/10.1148/radiol.2018181445 • Content codes: IR US

Purpose: To demonstrate the feasibility and safety of using focused ultrasound planning models to determine the treatment parameters needed to deliver volumetric mild hyperthermia for targeted drug delivery without real-time thermometry.

Materials and Methods: This study was part of the Targeted Doxorubicin, or TARDOX, phase I prospective trial of focused ultrasound–mediated, hyperthermia-triggered drug delivery to solid liver tumors (ClinicalTrials.gov identifier NCT02181075). Ten participants (age range, 49–68 years; average age, 60 years; four women) were treated from March 2015 to March 2017 by using a clinically approved focused ultrasound system to release doxorubicin from lyso-thermosensitive liposomes. Ultrasonic heating of target tumors (treated volume: 11–73 cm^3 [mean ± standard deviation, 50 cm^3 ± 26]) was monitored in six participants by using a minimally invasive temperature sensor; four participants were treated without real-time thermometry. For all participants, CT images were used with a patient-specific hyperthermia model to define focused ultrasound treatment plans. Feasibility was assessed by comparing model-prescribed focused ultrasound powers to those implemented for treatment. Safety was assessed by evaluating MR images and biopsy specimens for evidence of thermal ablation and monitoring adverse events.

Results: The mean difference between predicted and implemented treatment powers was −0.1 W ± 17.7 (n = 10). No evidence of focused ultrasound–related adverse effects, including thermal ablation, was found.

Conclusion: In this 10-participant study, the authors confirmed the feasibility of using focused ultrasound–mediated hyperthermia planning models to define treatment parameters that safely enabled targeted, noninvasive drug delivery to liver tumors while monitored with B-mode guidance and without real-time thermometry.

Online supplemental material is available for this article.

Focused ultrasound–mediated hyperthermia has long been studied as a noninvasive method of clinical targeted therapy, particularly for ablative applications (1–3). More recently, the use of ultrasound to induce "mild" hyperthermia (temperature elevations ≤6°C) has been investigated preclinically for targeted drug delivery through thermally triggered release from liposomal carriers (4–7). For clinical therapeutic focused ultrasound systems, MRI and B-mode US methods are the leading guidance techniques (8). The latter can indicate bubble formation as a hyperechoic region but does not provide thermal metrics. Alternatively, MRI guidance offers real-time thermometry superimposed on cross-sectional anatomic information, facilitating integration into treatment planning and control systems (9,10). The application of MRI-guided focused ultrasound systems is limited primarily by cost and, to a lesser extent, technical issues with motion and monitoring in adipose tissue (11,12).

In its simplest form, treatment planning for therapeutic ultrasound procedures employs diagnostic imaging to identify the treatment target and obstacles in the propagation path (13,14). Mathematic simulations allow prediction and optimization of physiologic and biologic responses, including acoustic pressure, corresponding temperature elevation (15–18), and drug delivery (19). Simulations may also greatly extend the understanding of the processes that occur during treatment (20).

The purpose of this study was to assess the clinical feasibility and safety of using computational planning

Summary

In this phase I study, it was feasible and safe to thermally trigger drug release over oncologically relevant volumes by using extracorporeally applied US-guided focused ultrasound, with treatment plans based on patient-specific modelling.

Implications for Patient Care

- Application of focused ultrasound to current and emerging oncology therapeutics could significantly improve their intratumoral dose and distribution for a given systemic dose.
- The pairing of acoustic and thermal planning models with low-cost B-mode US-based treatment guidance techniques has the potential to enable safe and effective focused ultrasound hyperthermia treatments to trigger and enhance drug delivery.

models to determine ultrasound parameters that facilitate release from thermally sensitive liposomes in the absence of real-time thermometry. This approach was motivated by the desire to investigate procedures that may ultimately be more broadly accessible and simpler to administer compared with those that employ MRI guidance.

Materials and Methods

The Targeted Doxorubicin, or TARDOX, study (ClinicalTrials.gov identifier NCT02181075) was a phase I clinical trial conducted under regulatory and ethical approval from the Health Research Authority National Research Ethics Service, the Oxford University Hospitals Research & Development Department, and the United Kingdom's Medicines and Health Care Products Regulatory Agency. Clinical protocol and oncologic outcome details are available elsewhere (21,22). Written informed consent was obtained before study-specific procedures were performed.

TARDOX was a prospective nonrandomized cohort study with the aim of determining the feasibility, safety, and potential efficacy of drug delivery to solid liver tumors triggered by focused ultrasound–mediated hyperthermia. The therapeutic agent consisted of doxorubicin encapsulated within a lyso-thermosensitive liposome (ThermoDox; Celsion, Lawrenceville, NJ), which was systemically administered at 50 mg/m^2 for 30 minutes (39.5°C release threshold). Celsion provided ThermoDox at no cost to the trial. The authors had control of the data and the information submitted for publication.

The study consisted of two parts, which were primarily differentiated by the use of real-time thermometry. For part I, direct monitoring of tumor temperature was performed with use of an implanted device (Cool-Tip E-Series 18-gauge thermistor [Covidien, Mansfield, Mass] or Accu5i 18-gauge thermocouple [Angiodynamics, Latham, NY]) inserted through a coaxial needle that also enabled biopsy collection. Part II of the study was performed without the use of thermometry. All participants were imaged with contrast material–enhanced MRI, contrast-enhanced CT, and fluorine 18 fluorodeoxyglucose PET/CT 1 day before, 2 weeks after, and 4 weeks after intervention to enable radiologic assessment of therapeutic response, with an additional MRI examination performed 1 day after treatment to assess for instantaneous thermal ablation. Treatment was performed with the participant under a general anesthetic, and high-frequency jet ventilation was used to reduce respiratory motion of the liver. Participants are identified in this article by study part (I or II) and index—for example, II.03 indicates the third patient treated with the part II protocol.

Inclusion criteria were a life expectancy of at least 3 months, at least one liver tumor measuring 1 cm or larger, and a left ventricular ejection fraction of at least 50%. Exclusion criteria included radiation therapy to the target region in the preceding

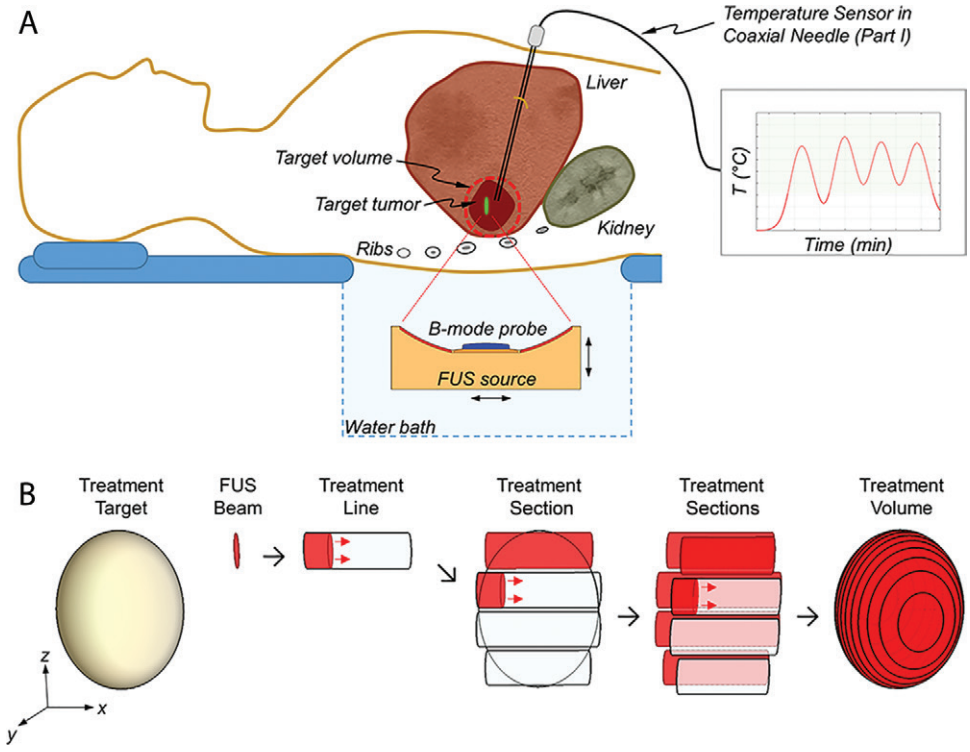

Figure 1: *A*, Diagram of treatment concept. In trial part I (six participants), target temperature elevation resulting from focused ultrasound (*FUS*)–generated heating was monitored with a thermometry device implanted through a coaxial needle that was also used for biopsy collection before and after focused ultrasound exposure. In part II (four participants), no thermometry device was used, and a single biopsy was performed after focused ultrasound treatment. *B*, Diagram illustrates target tumor volume coverage. A focused ultrasound (*FUS*) beam is moved along a line in linear mode, translating proximally to form a "section," then treating the target with multiple sections for complete volumetric coverage.

Table 1: Summary of Demographic and Tumor Characteristics

	Demographic Characteristics			Tumor Treatment Data		
Participant No.	Age (y)	Sex	BMI (kg/m^2)	Treated Volume (cm^3)	Diagnosed Tumor Type	Location (Segment)*
I.01	50	M	22.6	11	Diffuse multilobular hepatocellular carcinoma	VI
I.02	68	F	22.9	26†	Metastatic ductal breast carcinoma	V/VI
I.03	66	M	25.0	59†	Metastatic colorectal adenocarcinoma	V/VI
I.04	64	F	25.7	73	Metastatic colorectal adenocarcinoma	V/VI
I.05	49	M	26.3	67†	Metastatic colorectal adenocarcinoma	VI
I.06	65	M	25.9	52	Metastatic colorectal adenocarcinoma	VI
II.01	53	M	37.3	41	Metastatic squamous cell lung cancer	VI
II.02	63	F	25.2	50	Metastatic colorectal carcinoma	V
II.03	53	F	27.0	31	Metastatic colorectal adenocarcinoma	VIII
II.04	65	M	27.0	54	Metastatic colorectal adenocarcinoma	VIII

Note.—Part I was performed with invasive thermometry, and part II was performed without thermometry. Participants are identified in this article by study part (I or II) and index—for example, II.03 indicates the third patient treated with the part II protocol. BMI = body mass index.

* Liver segments were defined by using the Couinaud classification system.

† Time-averaged over the treatment.

12 months, a lifetime dose of doxorubicin of more than 450 mg/m^2, or another serious illness within the previous 6 months. Further details on the inclusion and exclusion criteria are provided in the protocol (22).

Treatment Parameters

Focused ultrasound was administered by using a clinically approved extracorporeal system (JC200; Chongqing Haifu, Chongqing, China). Focused ultrasound was produced by a single-element focused transducer (0.96 MHz) with a central opening that housed a B-mode US probe for treatment guidance and monitoring (Fig 1, *A*). The focused ultrasound source and B-mode probe were integrated within a motorized system that translated in three Cartesian coordinates and enabled scanning of the ultrasound beam to induce mild hyperthermia within a prescribed treatment volume.

Treatment planning required specification of ultrasonic (power, duty cycle) and geometric parameters, with the latter defining the spatial extents (depth, lateral, superior and/or inferior), speed, and sequence with which the focused ultrasound beam was moved. Treatment volume coverage (Fig 1, *B*) was specified in terms of lines (one-dimensional horizontal plane beam translation) and sections (sets of lines in a two-dimensional horizontal-depth plane).

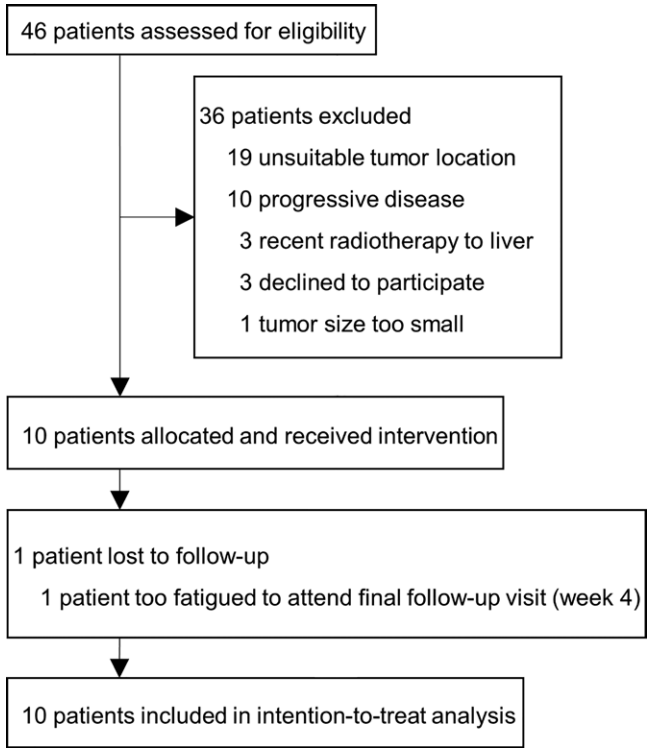

Figure 2: Diagram of study participant enrollment.

Treatment Planning Model

A model of ultrasound-induced hyperthermia was developed by using a combination of participant data and finite element calculations to specify focused ultrasound parameters and to estimate temperature fields for candidate treatment plans. Details are presented in Appendix E1 (online). Model inputs consisted of *(a)* participant anatomic data, *(b)* tissue acoustic and thermal properties, and *(c)* thermometric and radiologic results from the first two participants from part I. Tissue types and dimensions were determined from CT and MRI data after review (F.V.G., a senior radiologist with 23 years of experience; F.W., a focused ultrasound clinician with 16 years of experience, and P.C.L., a radiology clinical fellow) to identify a target tumor and a preferred intercostal route for extracorporeal focused ultrasound access. This information was used to construct three-dimensional acoustic and thermal models (M.D.G.). Model outputs for each participant were *(a)* a treatment recommendation (focused ultrasound power, duty cycle, and treatment volume) and *(b)* acoustic (pressure, intensity) and thermal (temperature, cumulative exposure) predictions. The final treatment

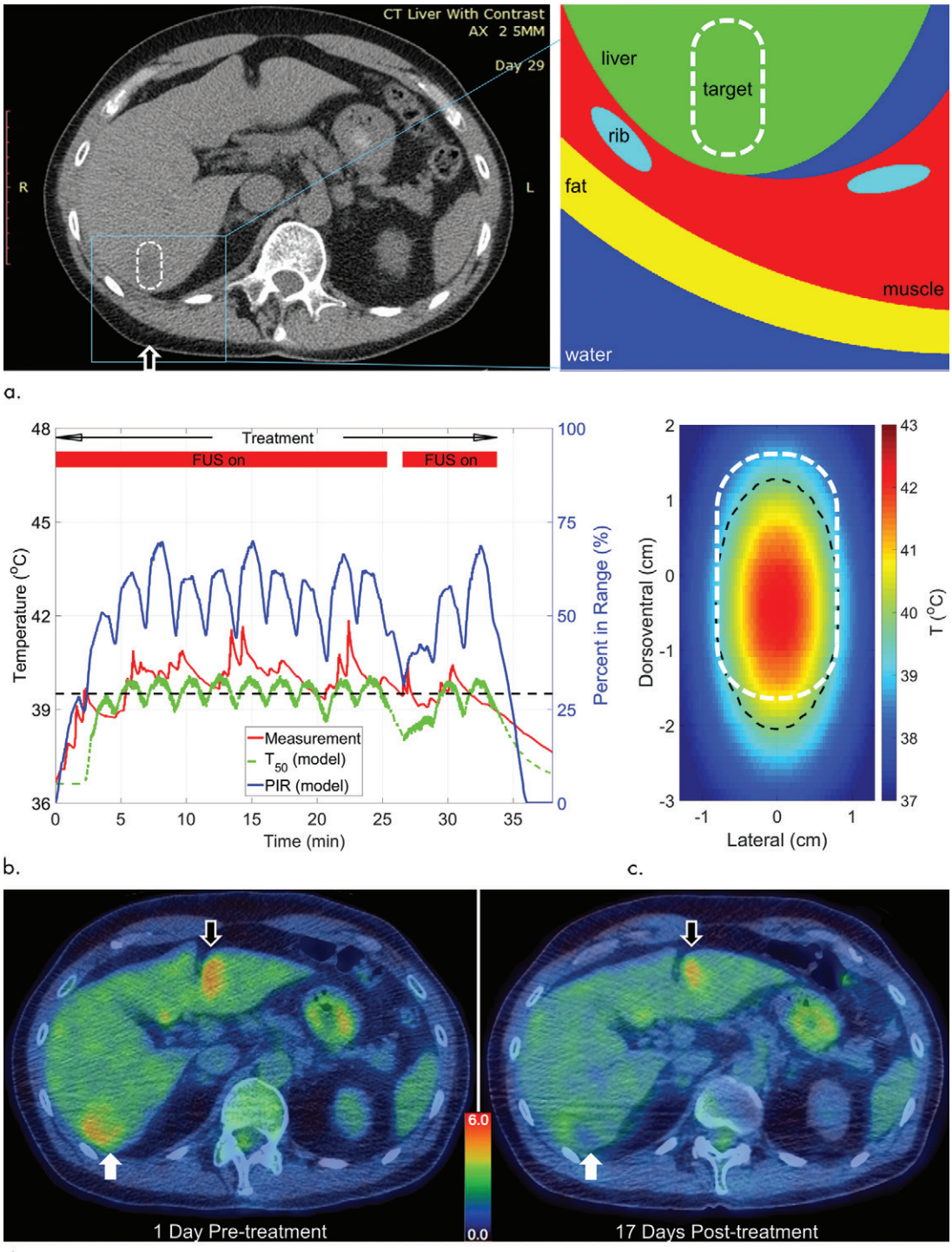

Figure 3: Treatment planning, modeling, and example results from participant I.01 (participant 1 from trial part I), a 50-year-old man with diffuse multilobular hepatocellular carcinoma in segment VI. **(a)** Left, axial contrast-enhanced CT scan with target tumor volume (white dashed line) and modeled region (blue box). Arrow indicates direction of incident focused ultrasound. Right, finite element model mesh transverse section corresponding to blue region in CT scan, with tissue classification labels. **(b)** Measured thermometry data accompanied by model calculations of treatment volume median temperature (T_{50}). The measurement and T_{50} prediction both lie close to the lyso-thermosensitive liposomal doxorubicin release threshold temperature of 39.5°C, which is indicated by black dashed line. *PIR* = percentage in range (portion of treatment volume between 39.5°C and 47°C). **(c)** Treatment median temperature (*T*) in midaxial transverse plane. Dashed white line indicates approximate treatment target boundary as in **a**. Black dashed line indicates a 39.5°C temperature contour. **(d)** Axial fluorine 18 fluorodeoxyglucose PET/CT images obtained 1 day before (left) and 17 days after (right) treatment. Total lesion glycolysis of target tumor (white arrows) decreased by 36.4% (21), whereas there was no substantial change over the volume of a similarly sized tumor that received drug but no focused ultrasound (black arrows). Color bar indicates standardized uptake value.

plan was decided by consensus (F.W., F.V.G., M.A., D.Y.F.C., P.C.L., M.D.G., C.C.C.).

Statistical Analysis

Equivalent continuous focused ultrasound powers (products of power and duty cycle) predicted for all study participants were compared with those used for treatment by the focused ultrasound clinician by using Bland-Altman graphical analysis and a paired *t* test calculated in GraphPad QuickCalcs (GraphPad Software, San Diego, Calif), with $\alpha = .05$. To provide physiologic context for the power predictions, custom Matlab scripts (MathWorks, Natick, Mass) quantified the median temperature, or T_{50} (23), corresponding cumulative equivalent minutes of exposure at 43°C, or CEM_{43}, and uniformity of heating in the treatment volume.

Results

Ten participants (six men aged 49–66 years [mean age, 58.0 years]; four women aged 53–68 years [mean age, 62.0 years]; overall age, 49–68 years [mean, 59.6 years]) were treated between March 2015 and March 2017 (Table 1, Fig 2). To illustrate the treatment planning methods, CT data, model generation, and resulting thermal predictions for participant I.01, are shown in Figure 3. The target volume was centered at a depth of 5.6 cm and treated, as indicated in the axial plane CT image (Fig 3a, left). The blue overlay denotes the region for which thermal and acoustic models were developed (Fig 3a, right).

Figure 3b shows the measured target tumor temperature along with the median temperature prediction. The measurement indicates a treatment average of 39.8°C, which closely matches the predicted treatment-averaged value (39.7°C) and suggests that the sensor measurement was representative of the median temperature in the targeted region. Thermal metrics describing the warmest 10% of the treatment volume at any

Table 2: Geometric and Focused Ultrasound Parameters

Participant No.	Midtarget Depth (cm)	Power (W)		Duty Cycle (%)		Equivalent Power (W)*	
		Model	Actual	Model	Actual	Model	Actual
I.01†	5.6	53	50	100	100	53	50
I.02†	8.5	70	70	100	100	70	70
I.03†	12.9	137	100	100	100	137	100
I.04	7.6	130	140	50	43‡	65	60‡
I.05	5.8	102	120‡	50	74‡	51	89‡
I.06	4.1	116	116	43	43	50	50
II.01	5.9	118	125‡	55	55	65	69‡
II.02	4.5	114	114	42	42	48	48
II.03	7.0	139	140	44	44	61	62
II.04	4.1	109	110	38	40	41	44

Note.— Participants are identified in this article by study part (I or II) and index—for example, II.03 indicates the third patient treated with the part II protocol. In-treatment parameter adjustments were made in five participants. In participant I.02, treatment began with a larger volume exposed in dot mode and ended with a smaller volume exposed in linear mode. In participant I.03, treatment depth span was reduced by one-third for the second and third coverage cycles. In participant I.04, duty cycle was modified between treatment cycles to assess temperature maintenance after initial heating. In participant I.05, after successful predrug infusion testing with model-prescribed parameters (50 W, 48 cm^3 volume), the target volume was expanded to treat over two intercostal spaces, then reduced over the subsequent treatment cycles. In participant II.01, power was elevated after the anesthesia system's indwelling esophageal thermometry indicated slightly low body temperature, requiring a higher focused ultrasound temperature elevation.

* Equivalent power was calculated by multiplying power by duty cycle.

† Model calculations were run retrospectively.

‡ Data were time-averaged over the treatment.

Table 3: Results of Thermometry

Participant No.	FUS Exposure Time (min)	T_{mean} (°C)		Cumulative Equivalent Minutes of Exposure at 43°C*†	PIR (%)†
		Sensor	Model		
I.01‡	33.2	39.8	39.7	0.5	52.2
I.02‡	74.6	39.3	39.4	2.1	51.1
I.03‡	72.4	38.9	38.3	0.1	26.2
I.04	66.0	41.5	40.1	2.3	46.4
I.05	80.0	40.1	38.4	0.2	27.6
I.06	64.5	40.6	40.9	5.7	55.0
II.01	55.1	…	41.7	29.2	57.4
II.02	69.8	…	39.6	1.0	49.5
II.03	74.6	…	41.7	21.7	60.0
II.04	72.9	…	39.4	0.6	47.6

Note.— Participants are identified in this article by study part (I or II) and index—for example, II.03 indicates the third patient treated with the part II protocol. Model-generated values were calculated on the basis of each actual treatment. FUS = focused ultrasound, PIR = percentage in range (portion of treatment volume between 39.5°C and 47°C), T_{mean} = temperature averaged over treatment time for the sensor and model (with use of the median of the treatment volume).

* Calculated for the median temperature in the treatment volume as a function of time.

† Model-generated values.

‡ Model calculations were run retrospectively.

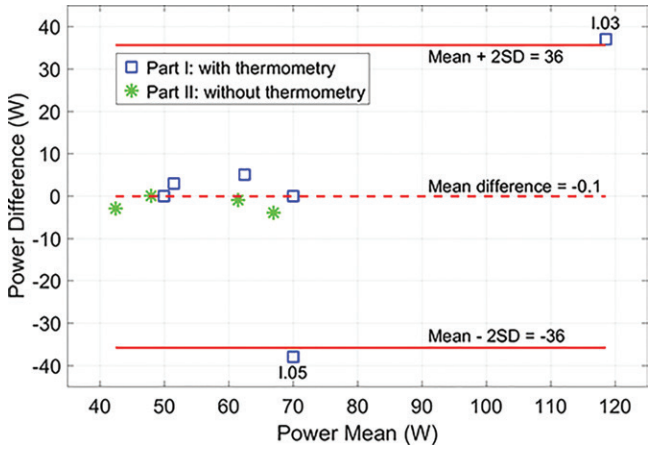

Figure 4: Bland-Altman display shows predicted and actual ultrasound powers. Mean difference in ultrasound powers (model power − actual power) was −0.1 W (n = 10). Standard deviation (*SD*) of ultrasound powers was elevated by two trial part I treatments: participant 3 (*I.03*), whose treatment was underpowered and shown to give suboptimal drug release (21), and participant 5 (*I.05*), whose treatment used a larger treatment volume than planned (see Table 2 footnote).

time (Appendix E1, section 8 [online]) indicated a low risk of ablative tissue damage. The right ordinate of Figure 3b quantifies the percentage of the treatment volume in the range of 39.5°–47.0°C (Appendix E1, section 4.6 [online]), demonstrating that at least half the prescribed volume is in the safe range for lysothermosensitive liposome release for 21.4 minutes.

The predicted temporal median temperature in the midaxial treatment plane shown in Figure 3c indicates that the region of temperature elevation was well-contained in the treatment volume, although it was proximally displaced by approximately 4 mm. This was primarily due to ultrasound beam refraction, which was accounted for in subsequent treatment plans.

PET/CT images in Figure 3d show a 36.4% reduction in total lesion glycolysis of the target tumor, whereas there was no substantial response over the volume of a similarly sized tumor (black arrows) that received the drug but no focused ultrasound (21). More broadly, partial responses were seen after a single treatment cycle in six of the 10 participants according to Choi criteria or PET Response Criteria in Solid Tumors, or PERCIST, with each modified for the target tumor alone (21).

The focused ultrasound treatment parameter data for each participant (Table 2) show that the prescribed power scaled approximately with target depth, subject to details of tissue morphologic characteristics. For the seven participants in whom model predictions were available at the time of treatment (participant I.04–I.06, participants II.01–II.04), the collective differences between predicted and treatment-averaged implemented powers were not significant clinically (mean, 3.5 W) and statistically (P = .33). These results indicate that the model consistently provided settings deemed safe by the attending radiologist and focused ultrasound clinician at the time of treatment and agree with the settings chosen in the presence of thermometry.

Models were run retrospectively for participants I.01–I.03, who were treated before model availability. The largest prediction discrepancy was seen with participant I.03, where the target depth was nearly 5 cm deeper than for any other participant. On the basis of thermometry (Table 3), the treatment for participant I.03 was substantially underpowered, and the use of the model-predicted settings (had they been available) should have improved target heating. Results of Bland-Altman analysis of the ultrasound power data for all 10 study participants (Fig 4) further reinforce the validity of the model based on a negligible bias (−0.1 W).

The measured and predicted thermometry data in Table 3 show that the measured treatment-averaged temperature in part I participants was within 0.1°–0.3°C of the model prediction (time average of median temperature) for the three participants with treatment volumes of 52 cm^3 or less (participants I.01, I.02, and I.06). The similarity of these temperatures also suggests that cavitation (24) was an unlikely heating mechanism. For participants with larger treatment volumes (participants I.04 and I.05), the time-averaged temperature prediction was 1.4°–1.7°C below the sensor-based value, suggesting that, as expected, the small sensor was not a good indicator of the median temperature of the larger targeted regions.

A review of histologic data (R.G., a histopathologist with 29 years of experience) and day 1 MRI data (F.V.G.) showed no clear evidence of instantaneous tissue ablation. Moreover, there were no skin burns, off-target tissue damage, or other clinically significant adverse effects related to focused ultrasound (21).

Discussion

The purpose of this study was to determine the clinical feasibility and safety of using computational planning models of focused ultrasound–mediated mild hyperthermia for targeted drug delivery. Feasibility was confirmed on the basis of the negligible mean difference between model-predicted and actual focused ultrasound powers (−0.1 W) required to achieve hyperthermia-mediated drug delivery, whereas safety was confirmed on the basis of a lack of focused ultrasound–related adverse effects. The proposed model-based treatment planning approach was demonstrated by comparing model and thermometry results (part I) and was safely extended to treatments without thermometry (part II). In addition, the model-prescribed treatments resulted in similar levels of enhanced drug delivery with or without real-time thermometry (21). These outcomes suggest that it may be feasible to pair planning models with low-cost (relative to MRI) monitoring techniques such as B-mode US, passive acoustic mapping (25), or US elastography (26) to guide and ensure the safety of nonablative treatments.

The performance of the treatment planning models in our study raises the question as to whether real-time monitoring of temperature for mild hyperthermia treatments will always be necessary to ensure safety and efficacy. For context, the equivalent continuous ultrasound powers (watts × duty cycle) used for moving focused ultrasound beam mild hyperthermia in the TARDOX study were 44–100 W (mean ± standard deviation, 64 W ± 18), whereas ablation procedures at comparable tissue depths have been carried out by using values as high as 450–545 W (27,28).

Chief among the limitations of our study was the small participant cohort. However, the study was designed for feasibility and safety assessments and was not intended to demonstrate

statistical significance. Thermometry data were recorded with a single stationary sensor, with potential errors arising from its presence in the acoustic field. However, this effect should be minimal over the majority of the treatment duration wherein the focused ultrasound beam is not directly impinging on the sensor (29). Lack of coregistration of ultrasound treatment with CT or MRI data limited the comparisons of temperature measurements and simulations.

To broaden the oncologic applicability of the radiology-based targeted drug delivery methods deployed in the TARDOX trial, systems should be scalable and deployable for numerous daily treatments in a single center. Such therapeutic scenarios should remove the need for anesthesia and high-frequency jet ventilation and include reduced-cost targeting and monitoring in place of bottleneck-inducing modalities.

Acknowledgments: The authors thank Celsion (Lawrenceville, NJ) for providing thermosensitive liposomal doxorubicin (ThermoDox) to the trial free of charge, and in particular Nicholas Borys, MD, for sharing his pre-clinical and clinical expertise on pharmacokinetics, characterization, and quantification of the drug in tissue and plasma.

Author contributions: Guarantors of integrity of entire study, M.D.G., M.R.M., C.C.C.; study concepts/study design or data acquisition or data analysis/interpretation, all authors; manuscript drafting or manuscript revision for important intellectual content, all authors; approval of final version of submitted manuscript, all authors; agrees to ensure any questions related to the work are appropriately resolved, all authors; literature research, M.D.G., P.C.L., C.M., R.G., C.C.C.; clinical studies, M.D.G., P.C.L., C.M., D.Y.F.C., S.S., M.A., R.G., F.W., M.R.M., F.V.G., C.C.C.; experimental studies, M.D.G., P.C.L., C.M., L.K.F., M.S., D.Y.F.C., R.C., C.C.C.; statistical analysis, M.D.G., R.C., C.C.C.; and manuscript editing, M.D.G., P.C.L., C.M., L.K.F., M.S., D.Y.F.C., S.S., M.A., R.G., R.C., M.R.M., F.V.G., C.C.C.

Disclosures of Conflicts of Interest: **M.D.G.** disclosed no relevant relationships. **P.C.L.** disclosed no relevant relationships. **C.M.** disclosed no relevant relationships. **L.K.F.** disclosed no relevant relationships. **M.S.** disclosed no relevant relationships. **L.C.** disclosed no relevant relationships. **D.Y.F.C.** disclosed no relevant relationships. **S.S.** disclosed no relevant relationships. **M.A.** disclosed no relevant relationships. **R.G.** disclosed no relevant relationships. **R.C.** disclosed no relevant relationships. **F.W.** disclosed no relevant relationships. **M.R.M.** Activities related to the present article: disclosed no relevant relationships. Activities not related to the present article: is a paid consultant for Amgen, Roche, GSK, Novartis, Immunocore, BMS, Eisai, Rigontec, BiolineRx, and Array; has grants/grants pending from Roche, AZ, GSK, Novartis, Millenium, Immunocore, BMS, Vertex, Eisai, Pfizer, Merck, Rigontec, Regeneron, Replimune, TCBiopharma, and Array; received travel/accommodations/meeting expenses unrelated to activities listed from Merck and Immunocore. Other relationships: disclosed no relevant relationships. **F.V.G.** disclosed no relevant relationships. **C.C.C.** Activities related to the present article: disclosed no relevant relationships. Activities not related to the present article: is paid to be on the board at OxSonics, OrthoSon, and OrganOx; is a paid consultant for OxSonics, OrthoSon, and OrganOx; institution receives payment for patents from OxSonics, OrthoSon, and OrganOx; institution receives royalties from OxSonics, OrthoSon, and OrganOx; has stock/stock options in OxSonics, OrthoSon, and OrganOx. Other relationships: has patents licensed to OxSonics and OrthoSon.

References

1. Fry WJ, Mosberg WH Jr, Barnard JW, Fry FJ. Production of focal destructive lesions in the central nervous system with ultrasound. J Neurosurg 1954;11(5):471–478.
2. Kennedy JE. High-intensity focused ultrasound in the treatment of solid tumours. Nat Rev Cancer 2005;5(4):321–327.
3. Hsiao YH, Kuo SJ, Tsai HD, Chou MC, Yeh GP. Clinical application of high-intensity focused ultrasound in cancer therapy. J Cancer 2016;7(3):225–231.
4. Hijnen N, Langereis S, Grüll H. Magnetic resonance guided high-intensity focused ultrasound for image-guided temperature-induced drug delivery. Adv Drug Deliv Rev I have2014;72:65–81.
5. Ponce AM, Vujaskovic Z, Yuan F, Needham D, Dewhirst MW. Hyperthermia mediated liposomal drug delivery. Int J Hyperthermia 2006;22(3):205–213.
6. Staruch RM, Ganguly M, Tannock IF, Hynynen K, Chopra R. Enhanced drug delivery in rabbit VX2 tumours using thermosensitive liposomes and MRI-controlled focused ultrasound hyperthermia. Int J Hyperthermia 2012;28(8):776–787.
7. Dromi S, Frenkel V, Luk A, et al. Pulsed-high intensity focused ultrasound and low temperature-sensitive liposomes for enhanced targeted drug delivery and antitumor effect. Clin Cancer Res 2007;13(9):2722–2727.
8. Ebbini ES, ter Haar G. Ultrasound-guided therapeutic focused ultrasound: current status and future directions. Int J Hyperthermia 2015;31(2):77–89.
9. Schlesinger D, Benedict S, Diederich C, Gedroyc W, Klibanov A, Larner J. MR-guided focused ultrasound surgery, present and future. Med Phys 2013;40(8):080901.
10. Kim YS. Advances in MR image–guided high-intensity focused ultrasound therapy. Int J Hyperthermia 2015;31(3):225–232.
11. Rieke V, Butts Pauly K. MR thermometry. J Magn Reson Imaging 2008;27(2):376–390.
12. Winter L, Oberacker E, Paul K, et al. Magnetic resonance thermometry: methodology, pitfalls and practical solutions. Int J Hyperthermia 2016;32(1):63–75.
13. Ranjan A, Jacobs GC, Woods DL, et al. Image-guided drug delivery with magnetic resonance guided high intensity focused ultrasound and temperature sensitive liposomes in a rabbit Vx2 tumor model. J Control Release 2012;158(3):487–494.
14. Hynynen K, Roemer R, Anhalt D, et al. A scanned, focused, multiple transducer ultrasonic system for localized hyperthermia treatments. Int J Hyperthermia 1987;3(1):21–35.
15. McGough RJ, Kessler ML, Ebbini ES, Cain CA. Treatment planning for hyperthermia with ultrasound phased arrays. IEEE Trans Ultrason Ferroelectr Freq Control 1996;43(6):1074–1084.
16. Botros YY, Volakis JL, VanBaren P, Ebbini ES. A hybrid computational model for ultrasound phased-array heating in presence of strongly scattering obstacles. IEEE Trans Biomed Eng 1997;44(11):1039–1050.
17. Gélat P, Ter Haar G, Saffari N. A comparison of methods for focusing the field of a HIFU array transducer through human ribs. Phys Med Biol 2014;59(12):3139–3171.
18. de Greef M, Schubert G, Wijlemans JW, et al. Intercostal high intensity focused ultrasound for liver ablation: the influence of beam shaping on sonication efficacy and near-field risks. Med Phys 2015;42(8):4685–4697.
19. Gasselhuber A, Dreher MR, Partanen A, et al. Targeted drug delivery by high intensity focused ultrasound mediated hyperthermia combined with temperature-sensitive liposomes: computational modelling and preliminary in vivo validation. Int J Hyperthermia 2012;28(4):337–348.
20. Lagendijk JJW. Hyperthermia treatment planning. Phys Med Biol 2000;45(5):R61–R76.
21. Lyon PC, Gray MD, Mannaris C, et al. Safety and feasibility of ultrasound-triggered targeted drug delivery of doxorubicin from thermosensitive liposomes in liver tumours (TARDOX): a single-centre, open-label, phase 1 trial. Lancet Oncol 2018;19(8):1027–1039.
22. Lyon PC, Griffiths LF, Lee J, et al. Clinical trial protocol for TARDOX: a phase I study to investigate the feasibility of targeted release of lyso-thermosensitive liposomal doxorubicin (ThermoDox®) using focused ultrasound in patients with liver tumours. J Ther Ultrasound 2017;5(1):28.
23. Leopold KA, Dewhirst M, Samulski T, et al. Relationships among tumor temperature, treatment time, and histopathological outcome using preoperative hyperthermia with radiation in soft tissue sarcomas. Int J Radiat Oncol Biol Phys 1992;22(5):989–998.
24. Coussios CC, Roy RA. Applications of acoustics and cavitation to noninvasive therapy and drug delivery. Annu Rev Fluid Mech 2008;40(1):395–420.
25. Jensen CR, Ritchie RW, Gyöngy M, Collin JRT, Leslie T, Coussios CC. Spatiotemporal monitoring of high-intensity focused ultrasound therapy with passive acoustic mapping. Radiology 2012;262(1):252–261.
26. Brosses ES, Pernot M, Tanter M. The link between tissue elasticity and thermal dose in vivo. Phys Med Biol 2011;56(24):7755–7765.
27. Peek MCL, Ahmed M, Napoli A, et al. Systematic review of high-intensity focused ultrasound ablation in the treatment of breast cancer. Br J Surg 2015;102(8):873–882; discussion 882.
28. Xie B, Zhang C, Xiong C, He J, Huang G, Zhang L. High intensity focused ultrasound ablation for submucosal fibroids: a comparison between type I and type II. Int J Hyperthermia 2015;31(6):593–599.
29. Lyon PC. Targeted release from lyso-thermosensitive liposomal doxorubicin (ThermoDox) using focused ultrasound in patients with liver tumours [doctoral thesis]. Oxford, England: University of Oxford, 2016.